# Self-Mixing Interferometer with a Laser Diode: unveiling the FM channel and its advantages respect to the AM channel

Silvano Donati, *Life Fellow, IEEE,* and Michele Norgia*, IEEE Senior Member*

***Abstract*—In a self-mixing interferometer (SMI) based on a diode laser, the measurement of the external reflector displacement s(t) is carried out by looking at the optical-phase signal cos 2ks(t), a signal readily detected as an amplitude modulation (AM) of emitted power. In contrast, the other available signal, sin 2ks(t), a frequency modulation (FM) of the emitted field at optical frequency, is never used because difficult to recover. Recently, Contreras et al. used a narrow-band acetylene cell to convert the FM into an amplitude signal, finding it is larger and has a better SNR than the AM. In this paper, we analyze the advantages of the new CFM (converted-FM) signal, calculating both amplitude and SNR, and compare theoretical results to published experimental evidence, finding good agreement. We then present options for realizing the selective filter in different configurations and technology. Finally, we evaluate the improvement offered by CFM in a number of measurements, like sub-wavelength vibrations, digital readout displacement, and diode laser alpha factor.**

***Index Terms* — Optical interferometers, Measurements, Optical feedback, Semiconductor laser diodes.**

## I. Introduction

Self-mixing interferometry (SMI) was introduced about 40 years ago [1], but only recently it has attracted much interest because it is based on a very simple configuration, as shown in Fig.1, and yet it is powerful tool in a variety of applications (see for example Ref.[2] for a review).

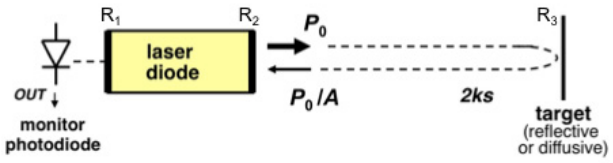


Fig.1 Schematic of a self-mixing interferometer (SMI) using a laser diode to sense the phase shift *2ks* of field returning from an external reflector (or diffuser) at a distance s.

The most developed application of SMI is the measurement of displacements, vibrations, and related kinematic quantities [2-4]. Additionally, other features of the SMI signal, for example amplitude, have been used to develop echo detectors [5,6] up to THz frequency [7,8], while waveform details have been used to measure a variety of quantities like e.g., index of refraction [9], line-width [10] and alpha factor [11-13] of the laser. The still growing areas of application of SMI span from device engineering [14,15] to biomedical [16,17] to consumer [18].

A laser diode is the most common optical source employed in the SMI (Fig.1) because it is compact and easy to operate, and usually carries a monitor photodiode (PD) in the same package The PD readily provides the readout of the signal $P=P_0 (1+m \cos 2ks)$ amplitude modulated (AM) by the phase shift $\phi=2ks$ (k being the wave-vector and s the target distance), just like in a normal interferometer.

The AM signal alone, however, has a problem of ambiguity in the measurement of displacement s(t), because of the non-monotonic cosine function. Several approaches have been devised to overcome the ambiguity, like phase unfolding [4], operation on external cavity mode switching [19], added phase modulation [20], etc.

Additionally, a simpler and more elegant solution consists in using also the other SMI signal generated together with the AM in the SMI interaction, the sin 2ks of frequency modulation (FM), because the cos2ks and sin2ks pair allows to trace back unambiguously the phase 2ks, as demonstrated in a seminal paper [1]. Impressed on the optical frequency, the FM signal is hard to detect in a diode laser SMI, whereas it can be readily recovered in a dual-mode He-Ne laser [1].

This because the He-Ne mode is easily split by the Zeeman effect into two orthogonal-polarized modes, spaced in frequency by MHz's and well decoupled from one another. One mode is kept inside the cavity so that it is unperturbed and serves as a local oscillator, while the other is allowed propagating to the target and collect the AM/FM modulations of the self-mix interaction. By beating the two modes at the photodetector, the AM and FM signals are down-converted from optical to electrical frequencies where they can be processed with standard electronics. This mode of operation, that leads to unambiguous measurement of displacement s(t) in $\lambda/2...\lambda/8$ steps (digital mode), and down to nm-resolution (analog mode), has unfortunately no counterpart in a diode laser because no mechanism for two-mode operation has been found, capable of supplying decoupled and frequency offset modes without introducing excessive burden.

Another interesting feature, the FM signal is much larger and may also have a better SNR than the AM signal, so it may be advantageous to use it even alone, when available, for a potentially improved measurement.

Manuscript received.....revised.....accepted..... S.Donati is with the Department of Industrial and Information Engineering, University of Pavia, v. Ferrata 1, 27100 Pavia, Italy. M.Norgia is with DEIB, Politecnico di Milano, p.za L. da Vinci 1, 20133 Milano. Corresponding author: silvano.donati@ieee.org

Recently, Contreras et al. [21] reported the detection of the FM signal in a semiconductor laser tuned to the edge of the P-branch line of acetylene, at $\lambda_P$=1531.58 nm. Thanks to the frequency selectivity, frequency deviations of self-mixing signal are translated into amplitude variations, resulting in a signal with a surprising increase of both amplitude (x1000) and SNR (x100) respect to the AM.
Of course, the laser wavelength had to be finely tuned to the edge of the resonance to exploit the maximum of the FM-to-AM conversion, requiring either a temperature or a drive current tuning. For ease of operation, it would be preferable to have to tune a filter to the laser line rather than the laser on the filter fixed-λ line, like demonstrated in a recent paper, Ref. [22], using a filter based on a Mach-Zehnder interferometer.

This paper is organized as follows: in Sect. II we present a quantitative analysis of the AM and FM signals based on the Lang and Kobayashi equations, and calculate signal amplitude, signal-to-noise ratio and improvement factors of the FM-to-AM conversion. In Sect. III we compare results of the analysis to experimental data of [22]. Then, in Sect. IV, we consider the options for implementation of the λ-selective element, and in Sect. V develop their all-fiber and micro-optics versions and discuss their design. Last, in Sect. VI we present three examples of applications in which the CFM signal can offer a novel approach to develop SMI instrumentation with improved performance.

## II. ANALYSIS

The SMI system of Fig.1 is modeled by well-known Lang-Kobayashi equations [2,23], written as:

$$dE/dt = ½ [G_N(N- N_0)-1/\tau_p] E + (K/\tau_{in}) E(t-\tau_{ext})\times \times \cos [\omega_0\tau_{ext} +\phi(t)- \phi(t-\tau_{ext})]$$

$$d\phi/dt = ½ \alpha\{G_N(N-N_0)-1/\tau_p\} + (K/\tau_{in}) E(t-\tau_{ext})/E(t)\times \times \sin [\omega_0\tau_{ext} +\phi(t)- \phi(t-\tau_{ext})]$$

$$(d/dt)N = J\eta/ed - N/\tau_r - G_N(N- N_0) E^2(t) \qquad (1)$$

where:
$G_N$ = modal gain = $8.1\cdot10^{-13}$ m$^3$s$^{-1}$,
K = $\eta_s (1-r_2^2)(r_3/r_2)$ fraction of field coupled into the oscillating mode, in terms of mirror (field) reflectivity (Fig.2), and mode superposition factor $\eta_s$,
$r_2$ = output mirror (field) reflectivity = 0.59 typ.
$\eta_s$ = mode superposition (field) factor = $\eta_m \lambda/\pi w_t$, product of mode distribution factor $\eta_m$ (typ.=0.5) and of geometrical (field) attenuation $\lambda/\pi w_t$, as derived by acceptance invariance [23],
$w_t$ = spot size at the target, =$[\lambda s/\pi]^{1/2}$ as a diffraction-limited value with a focusing objective, or $w_t$ = sθ for a free space propagation with divergence θ (=$\lambda/\pi w_0$),
N = carrier concentration (m$^{-3}$),
$N_0$ at inversion =$1.2\cdot10^{24}$ m$^{-3}$,
$\tau_{ext}$ =2ns/c = round trip time of external cavity
s = distance to external cavity reflector,
2ks = external optical phase shift
$\tau_{in}$ =2n$L_{in}$/c = round trip time of laser cavity, =2...5 ps, typ.
$\tau_p$ = photon lifetime in laser cavity, =5...10 ps, typ.
$\tau_r$ = carrier lifetime = 2 ns, typ.
α = line width enhancement factor, (taken 3 ... 6)
$\omega_0$ = k/c = unperturbed frequency ($\lambda_0$= 1.55 μm)
$\omega_0\tau_{ext}$ =2ks
Jη = pumping current density, and
η = internal quantum efficiency
d = active layer thickness
V = active volume = $8\cdot10^{-17}$ m$^3$

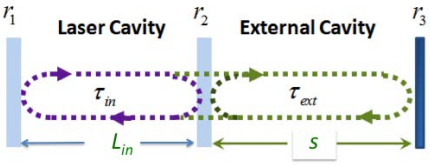

Fig.2. Layout of an SMI and associated quantities.

Also introduced is the C-factor [1-3] given by:

$$C = (1+\alpha^2)^{1/2} \eta_s K (\tau_{ext}/\tau_{in}) \qquad (2)$$

In this notation, K accounts for the mirror and geometrical losses, and $\eta_s$ for the mode-distribution mismatch.
With the above values, the threshold current is $I_{thr}$=11 mA, and in simulations it is convenient to assume a moderate overdrive factor, e.g. $J/J_{thr}$ =1.36 so that J=15 mA.

Self-mixing theory [2,5] predicts that the AM modulation index (or amplitude ΔE) is proportional to cos 2ks at small K, whereas the FM modulation index (or frequency deviation Δν) is proportional to sin (2ks+atan α).

These results are readily found from L-K equations (Eq.1), on letting K<<1 and developing [3,4] field amplitude and phase in the small signal regime as E= $E_0$+ΔE, and ω=dφ/dt=$\omega_0$ +Δω, where $E_0$ and $\omega_0$ are the quiescent values obtained for dE/dt=0, dφ/dt=0. Doing so, we find:

$$\Delta E = [E_0 \kappa C \cos 2ks] / [1+ C \cos 2ks],$$

where $\kappa= (1+\alpha^2)^{-1/2}\tau_p/\tau_{ext}$ (3A)

$$= E_0 \kappa C \cos 2ks \quad \text{for } C<<1, \text{ and} \qquad (3B)$$

$$\Delta\omega = - (C/\tau_{ext}) \sin (2ks +\text{atan } \alpha)/(1+C \cos 2ks)$$

$$= - (C/\tau_{ext}) \sin (2ks +\text{atan } \alpha) \quad [\text{for } C<<1] \qquad (4)$$

Thus, for C<<1, both modulations are sinusoidal, and are phase-shifted of the difference arg(ΔE)-arg(Δν)=ζ of the sine and cosine function. Looking at Eqs.3 and 4 we get:

$$\zeta= \pi/2-\text{atan } \alpha \qquad (5)$$

When α is small (≈0), like for a He-Ne laser, ζ≈π/2 and the AM and FM signals constitute a nice orthogonal pair of signals, i.e., sin2ks and cos2ks [1], from which it is relatively easy to trace back the displacement s(t) unambiguously [1]. On the contrary, in semiconductor lasers the large α-factor brings the AM and FM signals closer to in-phase condition. Yet we can still apply the same processing of He-Ne, although with some loss in SNR, by converting the AM and FM signals into an orthogonal pair, as shown in Sect. VIb.

*II a- Signal Amplitudes*

From Eqn.3 and 4, the (peak) amplitudes of the AM and FM signals are, for small C:

$$\Delta E_p = E_0\, \kappa C, \qquad \Delta\omega_p = C/\tau_{ext} \tag{6}$$

Now, let us write the detected power $P_0$ of the SMI in unperturbed conditions as:

$$P_0 = E_0^2$$

where for simplicity a constant multiplicative factor $A/2Z_0$ [24] has been omitted. The power variation due to the AM signal is

$$\Delta P_{AM} = 2E_0\, \Delta E = 2P_0\, \kappa C \tag{7}$$

About the FM-to-AM converted signal, upon edge-filtering the FM signal with a filter of frequency response F(ν), a photocurrent variation is developed, given by the power $P_{out} = E_{out}^2$ multiplied by the filter slope $S_F$ and by the (peak) frequency deviation $\Delta\nu_p=\Delta\omega_p/2\pi$. Thus, the converted-FM (or CFM) signal is given by:

$$\Delta P_{CFM} = P_{out}\, S_F\, \Delta\omega_p/2\pi = P_{out}\, S_F\, C/2\pi\tau_{ext} \tag{8}$$

where $P_{out}$ may in general differ from power $P_0$. In Eq.8, the slope of the filter, $S_F = dF(\nu)/F(\nu)d\nu$, is approximately given by the inverse of half the filter line width, or $\sigma_F \approx (\Delta\nu_{filter}/2)^{-1}$, assuming F(ν) is normalized to unit area.

We define an amplitude gain $G_{FM\text{-}AM}$ of the FM-to-AM conversion of the SMI signal by edge filtering process, as

$$G_{FM\text{-}AM} = \Delta P_{CFM}/\Delta P_{AM} \tag{9}$$

Using Eqs.7, 8 and 3A, we obtain

$$G_{FM\text{-}AM} = [S_F\, (1+\alpha^2)^{1/2}/4\pi\tau_p]\, (P_{out}/P_0) \tag{10}$$

Note that, besides a trivial power ratio, the gain only depends on photon lifetime $\tau_p$ and alpha-factor $\alpha$ for a given laser.

*II b - Signal-to-Nose Ratio*

Let's start evaluating the noises associated to the AM and FM signals. About the amplitude signal $\Delta P_{AM}$ (Eq.7), the dominant contribution in the coherent process of SMI signal detection is the shot noise of the large (unperturbed) component $E_0$. This noise has a rms value given by [4,24]:

$$p_{nAM} = (2h\nu P_0 F_n B)^{1/2} \tag{11}$$

where $P_0$ is the power of the AM signal, and $F_n$ stands for the excess noise factor respect to the quantum noise limit ($F_n$= RIN/[$P_0$/2hνB]), inclusive also of the quantum efficiency loss $1/\eta_q$ of the detector). Using Eq.7 with $E_0^2=P_0$, the SNR, understood as the ratio of peak-signal to rms noise is:

$$SNR_{AM} = 2\, \kappa C\, [P_0/2h\nu F_n B]^{1/2} \tag{12}$$

or, the SNR of the AM channel is 2κC times the value of the SNR associated to the detection of power $P_0$. Using Eqs.2 and 3A we can also express Eq.12 as:

$$SNR_{AM} = 2\, \eta_s K\, (\tau_p/\tau_{in})\, [P_0/2h\nu F_n B]^{1/2} \tag{12A}$$

or also:

$$SNR_{AM} = 2\, \eta_s K\, (\tau_p/\tau_{in})\, SNR_{P0} \tag{12B}$$

where we have let $SNR_{P0} = [P_0/2h\nu F_n B]^{1/2}$ for the signal-to-noise ratio of power $P_0$ measurement.

About noise of the FM channel, we start from the well known Schawlow-Townes line width [25,26], in the version written with a ½ correction factor introduced by Lax [27] as:

$$\Delta\nu_{S\text{-}T} = \tfrac{1}{2}\, g\, 4\pi\, h\nu\, \Delta\nu_{cav}^2/P_{out} \tag{13}$$

where $\Delta\nu_{cav}$ is the cavity line width, half-width half-maximum (HWHM), $\Delta\nu_{S\text{-}T}$ is also a HWHM line width, $g=N_2/(N_2-N_1)$ is the spontaneous emission factor (g≈1 above threshold), and $P_{out}$ the power emitted from the laser.

In the following, we assume g≈1, and let in Eq.13 $2\Delta\nu_{cav}=1/2\pi\tau_p$ to express [28, 29] the full-width half-maximum (FWHM) line width $2\Delta\nu_{cav}$ in terms of photon lifetime $\tau_p$, and finally multiply by the line width enhancement factor $1+\alpha^2$ of the semiconductor laser [25-30] obtaining for the Schawlow-Townes line width $\Delta\nu_{n0}$:

$$\Delta\nu_{n0} = (1+\alpha^2)\, h\nu\, (P_{out}\, 8\pi\, \tau_p^2)^{-1} \tag{14}$$

Note that this result is independent from bandwidth B or measurement time T.

We could think $\Delta\nu_{n0}$ is the frequency rms noise we are looking for, but this is a fallacy. Indeed, the Schawlow-Townes line-width of Eq.14 is the width of the frequency line (or, the standard deviation of the frequency *distribution*), while we need the *frequency noise* superposed to the frequency signal, which is the average frequency observed on an integration time T (or, over a measurement bandwidth B=1/2T), a quantity that will scale down as $1/\sqrt{T}$ or $\sqrt{B}$.

To take account of the integration, following P. Laurent et al. [31] we recall that the white noise spectral intensity S(Ω) of pulsation Ω=2πν, is 2 times the rms line-width $\Delta\Omega_{n0}=2\pi\Delta\nu_{n0}$. So, by expressing the spectral density of frequency as $S(\Omega)/(2\pi)^2$, multiplying it by B and taking the square root [32] we obtain for the contribution to frequency noise as:

$$\Delta\nu_{nI}=\sqrt{[2\Delta\Omega_{n0}/(2\pi)^2 B]} = \sqrt{(\Delta\nu_{n0} B/\pi)}.$$

Using Eq.14 the frequency noise rms contribution reads:

$$\Delta\nu_{nI} = (1+\alpha^2)^{1/2}\, [h\nu B/2P_{out}]^{1/2}\, (2\pi\tau_p)^{-1} \tag{14A}$$

[*Alternative derivation*: interesting to note, with a different approach we could had written directly $\Delta\nu_{nI} = \Delta\nu_{cav}/\sqrt{N}$ to represent that each photon samples the cavity line and introduces an uncertainty equal to $\Delta\nu_{cav}$ that scales down as $1/\sqrt{N}$ for N photons; and by substituting $\Delta\nu_{cav}=1/4\pi\tau_p$ and $N=(P_{out}T/h\nu)$ for the number of photons in the measurement time T =1/2B, we get the result $\Delta\nu_{nI} = [h\nu B/2P_{out}]^{1/2}\, (2\pi\tau_p)^{-1}$, which differs from Eq.14A only for the a-posteriori factor $(1+\alpha^2)^{1/2}$. Also interesting point, on reversing the steps of reasoning, from $\Delta\nu_{nI}=\Delta\nu_{cav}/\sqrt{N}$ we trace back the Schawlow-Townes line width given by Eq.13, with a new approach completely different from standard derivations, one that incidentally justifies the ½ correction of Lax].

*High level effects*: Eq.14A gives the frequency noise of an unperturbed, stand-alone laser.
But, when it is subjected to optical feedback, the line-width is affected and, as well known since early studies of optical feedback, it is either narrowed or broadened according to the phase of the returning field, in the regime II of the Tkach and Chraplyvy diagram (T-CD) [33]
(On the contrary, feedback has no extra effect on the amplitude noise $p_{nAM}$ [34,37]).
At increased coupling, the laser first returns to the single mode regime (the narrow region III of T-CD) then enters in the regime IV of coherence collapse where it breaks into period-1, multi-periodicity, and chaotic oscillations [38, 39].
Line narrowing/broadening has been extensively studied by Petermann [34-36] who found that the perturbed line-width $\Delta\nu_{pert}$, respect to the unperturbed $\Delta\nu_0$, is reduced by a factor:

$$\Delta\nu_{pert}/\Delta\nu_0 = [1+C\sin(2ks+\text{atan}\,\alpha)]^{-2} \qquad (15)$$

where as usual $2ks=2\pi\Delta\nu_{pert}\tau_{ext}$. From Eq.15, the maximum narrowing factor is $(1+C)^{-2}$ and is found at the external phase value $2ks+\text{atan}\,\alpha = \pi/2$, whereas the maximum gain is at $2ks=0$, for which the reduction factor is $(1+\kappa\tau/\tau_{in})^{-2}$ [37]. Similar results were found also by Agrawal [40] and Duan et al [41].

Interestingly, the laser will preferably lock at the minimum line-width rather than at the maximum gain [35-38], so that factor can $(1+C)^{-2}$ be assumed as the naturally occurring reduction of line-width and frequency rms deviation.
Actually, as noted by Schunk and Petermann [35], during a full $2\pi$-swing of the phase $2ks$, the laser may, at increasing C, enter into coherence collapse for a certain interval of phase $2ks$, with the line-width increasing to infinity [35-37] in simulations (see for example Fig.13 of Ref. [34]). In this regime, a period-1 or a multi-periodic, or a chaotic waveform is generated by the laser, as amply confirmed in literature [37,39].

Yet, the time scale of these coherence collapse waveforms is much shorter (because of the order of $1/f_2$, the upper frequency cutoff of the laser) than the time scale of the SMI measurement (ms, or at most, μs), so these oscillations are filtered out from the system frequency response, and don't disturb the operation of the much slower SMI waveform.

Indeed, the *average* value of field amplitude or phase in crossing a narrow coherence collapse region is found to be the same as in nearby stable states [42], as we have verified experimentally. Also the spectrum of frequency fluctuations at the unstable phase values corresponding to the coherence collapse is little influenced: experimentally the power density is found to increase, almost uniformly in frequency, of 20-50% when crossing the unstable regions [42] at C values up to 20...50. This statement may look surprising but doesn't contradict the previous analyses [33-37, 40-42] based on stability exponents, because relative to a different time scale, a slow one for SMI signals.
The reason why the SMI signals can coexist practically unaffected by the coherence collapse waveforms is out of the scope of this paper and will be treated in a separate study.

It's only when the entire space $(\kappa,2ks)$ is finally filled with unstable states, as found numerically [42], that we see experimentally random amplitude and phase switching and operation of the SMI is impaired.

So, in practice, we can conclude that the SMI can be operated up to C factors as high as 20…50 without incurring in any effect disturbing the operation of the measurement on ms or μs scale. Correspondingly, in the range C up to 20...50, we can assume the quantity $\chi(1+C)^2$ as the line-width narrowing, where $\chi$ = typ. 0.8-1.0 is an adjustment factor.
The narrowing impacts $\Delta\nu_{n0}$ as $\chi(1+C)^2$ and $\Delta\nu_{nI}$ as $(1+C)\sqrt{\chi}$ because of the argument leading to Eq.14A.
Then we can rewrite Eq.14A for the frequency rms fluctuation of the laser under optical feedback as:

$$\Delta\nu_{nI} = (1+\alpha^2)^{1/2}[h\nu B/2P_{out}]^{1/2}\,[2\pi\tau_p\sqrt{\chi}(1+C)]^{-1} \qquad (16)$$

Now, the SNR of the FM signal is found as the ratio of signal $\Delta\nu_p = C/2\pi\tau_{ext}$ (Eq.6) to noise $\Delta\nu_n$ of Eq.16. By considering that both signal and noise are converted into amplitudes by the same multiplicative factor $S_F$, the same ratio will hold also for the converted signal $SNR_{CFM}$ and thus we can write:

$$SNR_{CFM\text{-}I} = \sqrt{\chi}(1+C)\,C\,(\tau_p/\tau_{ext})\,(2P_{out}/h\nu B)^{1/2}(1+\alpha^2)^{-1/2}$$
$$= \sqrt{\chi}(1+C)\,\eta_s K\,(\tau_p/\tau_{in})\,(2P_{out}/h\nu B)^{1/2} \qquad (17)$$

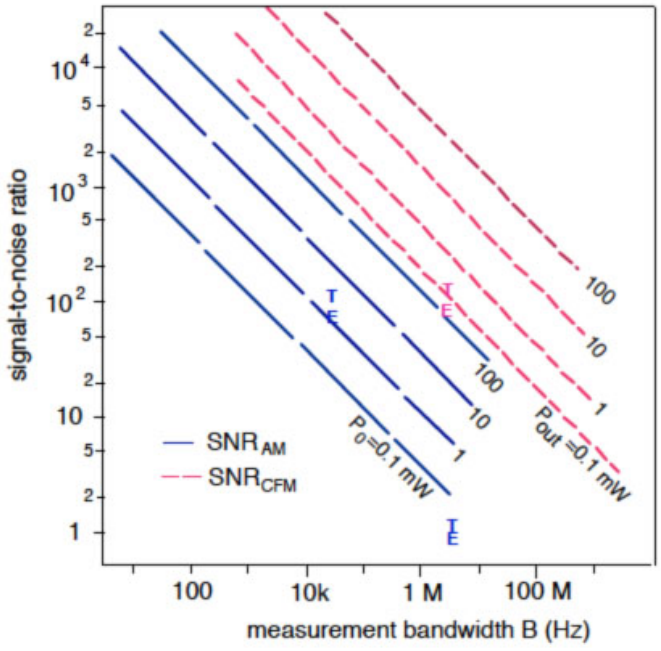


Fig.3 (color online) Signal-to-noise ratio of AM (blue dashed line) and CFM (red dotted line) channels plotted versus measurement bandwidth B and with powers $P_{out}$ and $P_0$ as parameters. Points E and T are experimental and theoretical pairs. Assumed values are: C=2, α=6, $F_n$=2, χ=0.8, $\tau_p$ = 4ps, $\tau_{in}$= 9ps, and $\tau_{ext}$=3.67 ns.

In Fig.3 we report the diagram of AM SNR ratio (Eq.12) and of the FM SNR (Eq. 17).

From the comparison, it turns out that the CFM signal behaves better than the AM especially at large bandwidth, where it can outperform the AM by more than one decade at equal used power.

## III. CHECK WITH EXPERIMENTAL DATA

An experimental validation of the interferometer filtering has been carried out as described in Ref. [22], using a DBF laser (Laser Wavespectrum WSLP-1550-008m-9-DFB), emitting 25-mW at $\lambda$ =1550-nm. An MZ-I filter was assembled in both the micro-optics and the all-fiber technology, to realize the off-line configuration (as explained later in Sect. IV).

In Eq.10 we now insert the slope value $S_F$ =19 GHz$^{-1}$ of the Mach-Zehnder filter [22], the power ratio $P_{out}/P_0$ = 0.08 resulting from the powers used in the CFM ($P_{out}$=0.8-mW) and AM ($P_0$ =10-mW) channels, and the estimated values of $\tau_p$= 4 ps for the DFB laser. Then, for $\alpha$=6 we obtain from Eq.10 a gain $G_{FM-AM}$=91, in reasonable agreement with the experimental value of 70 found in [22].

Note that if the full power were used in the CFM channel, the gain would have increased to $G_{FM-AM}$ =1127, a value comparable to that found in [21] using the acetylene cell as the frequency filter.

Further, to evaluate the SNR in Eqs.12 and 17, we take:

- mirror reflectivity $r_2^2$=0.5, and
- target reflectivity $r_3$=0.6 (estimated), so that
- coupling factor $K= r_3(1-r_2^2)/r_2 = 0.434$
- $\tau_p$ =4-ps, $\tau_p/\tau_{in}=[-\ln(r_2 r_2)]^{-1}$ =1.44
- superposition factor $\eta_s=A^{-1/2}=\eta_m \lambda/\pi w_t=0.6 \cdot 1.53 \cdot 10^{-3}/3.14 \cdot 1.74 = 0.169 \cdot 10^{-3}$ ($\lambda/\pi w_t$ is the back trip attenuation for a spot $w_t$ at the target and $\eta_m$=0.6 the mode superposition),
- $\kappa = 0.179 \cdot 10^{-3}$
- laser power output $P_{out}$=20-mW, and AM channel power $P_0$= 5-mW
- measurement bandwidth B: AM, 28 kHz, and CFM, B=20 MHz
- excess noise factor $F_n=NF/\eta_q$ =2.5 (for a laser excess noise NF=2 and a detector quantum efficiency $\eta_q$=0.8)

Inserting these values in the above expressions gives: C=2.06 (a value consistent with the waveform of the SMI signal shown in Fig.2, Ref. [22]), and from Eq.12 $SNR_{AM}$=106 respect to the 70 found in the experiment [22].

About Eq.17, we find the theoretical value $SNR_{CFM-I}$ =117, to be compared to the measured value of 98.

In Fig.3 the pairs of theoretical and experimental points are reported as T's and E's.

Of course, having used estimated values of parameters, not measured ones, the match of calculated and experimental data can be regarded as more than satisfactory. Yet the values of $SNR_{AM}$ and $SNR_{CFM}$ can be reconciled by just taking a slightly different set of parameters like K, $\tau_p$, $\tau_{in}$, $\alpha$, and B.

However, the match cannot be much better than the order-of-magnitude, because the amplitudes of $\Delta P_{AM}$ and $\Delta P_{CFM}$ signals (Eqs.7 and 8) are valid in the small C approximation and are expected to saturate somehow at C>1. This partly explains why T's are consistently higher than E's in Fig.3.

With the factor $\chi$ introduced in Eq.17 we could take into account saturation, but this will be studied in a separate paper. From the results, it turns out that the important factors contributing to the improvement in SNR of the converted FM respect to the AM channel, are: (i) signal power $P_{out}$, and (ii) measurement bandwidth B. A relatively high value of power, such as the $P_{out}$=350-mW employed in Ref. [21] is the reason for the higher $SNR_{CFM}$ value found, whereas if we use a laser with a moderate power (say 3.5-mW) to mitigate laser safety issues, the gain in SNR drops to a one-digit figure, other parameters being unchanged.

## IV. SCHEMATICS FOR THE FM-CHANNEL SMI

Basically, there are two options for the implementation of the FM-channel SMI, according to the placement of the selective filter respect to the laser-to-target propagation path.

As shown in Fig.4, we can have: (i) an *in-line* SMI setup, when the filter is placed at the laser output and is crossed by the beam going to the target and back, or (ii) an *off-line* SMI setup when we create a separate path picking a fraction of the outgoing beam to feed the filter.

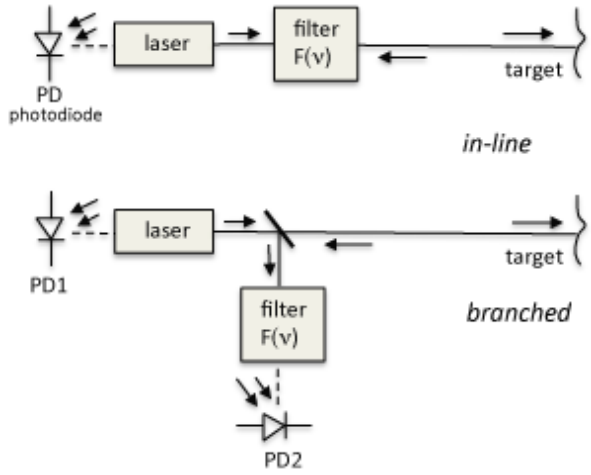


Fig.4. Two options for the FM-channel SMI: (top) *in-line* setup with the filter crossed by the laser beam along the go-and-return path, with the photodiode PD summing up the AM and CFM signals; (bottom) *off-line* setup, with the filter located off the propagation path and fed by a beam splitter, providing the AM channel at PD1 and the CFM channel at PD2.

In the first case we have available a larger power (and a better SNR), but the AM and the converted FM signals will be summed up into just one channel; to recover both AM and FM signals we shall be able to dither the filter in and out of the propagation path.

On the other hand, in the second case we have less power but can access simultaneously both the AM and the converted FM signals (at photodiodes PD1 and PD2, Fig.4), a feature useful for most applications (see Sect.VI).

Another crucial difference of the two schematics is about the reflection from the filter back into the laser: a strong reflection from the entrance surface (like, e.g., the case for a Fabry-Perot filter) can severely affect the laser of the in-line setup, whereas

in the branched setup we can insert an optical isolator before the filter and cut the reflection off.

About the way a retro-reflection can affect the laser in the in-line setup, we shall consider two mechanisms: (i) changes of the optical phase of the returning field and (ii), strong power injection into the laser cavity.

Writing the distance $d_F$ to the filter entrance mirror as the sum of a constant part plus a time-varying term, $d_F = d_{F0} + \Delta d_F(t)$, we see that phase $k\Delta d_F(t)$ is actually a spurious self-mixing signal. This signal is usually picked up unintentionally because of the micro-phonics sensitivity to ambient vibrations of the laser-and-filter mechanical assembly. Of course, we need to ensure $k\Delta d_F(t) \ll 1$ [i.e., $\Delta d_F(t)$ much less than a small fraction of $\lambda$] through a suitable mechanical design of the assembly, sturdy and immune to vibrations from the ambient.

The second contribution, a constant power reflected back into the cavity, may simply entail a change of emitted power, when the distance $d_{F0}$ is small (less than a few cm), as explained in Ref. [43] where the dependence of power on the tilt angle of input filter mirror respect to output laser mirror is also unveiled. In the case of simultaneous large reflections and large distances even a constant power back-reflected into the cavity may drive the laser to the high-dynamics regimes of multi-periodicity and chaos [33-35]. Yet these regimes are avoided when the distance to the filter is kept small (a few cm or less) and the mechanical mount is made stiff enough to become insensitive to ambient vibrations. So, in principle, all the *in-line* configurations of Fig.5 can be implemented.

## V. FILTERS

For the FM-to-AM conversion to be effective, we need a relatively narrow-line filter: from the results of Sect. II we need typically a line-width $\Delta\lambda_F \approx 5...10$-pm (FWHM) or a slope $\sigma_F \approx 1.5...3$ GHz$^{-1}$, as mentioned in Sect. III.

We have three possible technologies to implement the filter: (i) absorption lines of gases; (ii) grating filters; (iii) interferometers. An example of option (i) is the acetylene cell line at 1531.58 nm used in Ref. [21], while Ref. [44] is an example for (ii). However, in case (i) the selectivity is at a fixed wavelength that may not be reasonably close to the laser tuning range, thus restricting practical applicability, and in case (ii) wavelength can be the tuned by tilting the (bulk) filter or stretching the fiber (in a Fiber Bragg Gratings).

About (iii), any of the well-known interferometer schemes used in electro-optical instrumentation [4] and optical fiber sensors can be employed to make the FM-to-AM conversion, like e.g. Fabry-Perot (FP-I), Sagnac Ring (SR-I), Michelson (M-I) and the Mach-Zehnder (MZ-I) interferometer of [22].

The schematics of these interferometers, drawn in the bulk-optics version suitable for in-line setup are reported in Fig.5.

The output response $P(\nu)$ of the M-I and MZ-I to an input power $P_0$ is written as:

$$P(\nu) = P_0 (1+\cos 2\pi\nu\Delta L n/c) \qquad (19A)$$

where $\Delta L = L_1 - L_2$ is the difference between the length of the two arms for the MZ-I, and $\Delta L = 2(L_1 - L_2)$ for the M-I. Differentiating P respect to $\nu$ at middle of the fringe yields a slope:

$$S_F = 2\pi (n\Delta L/c) \qquad (20A)$$

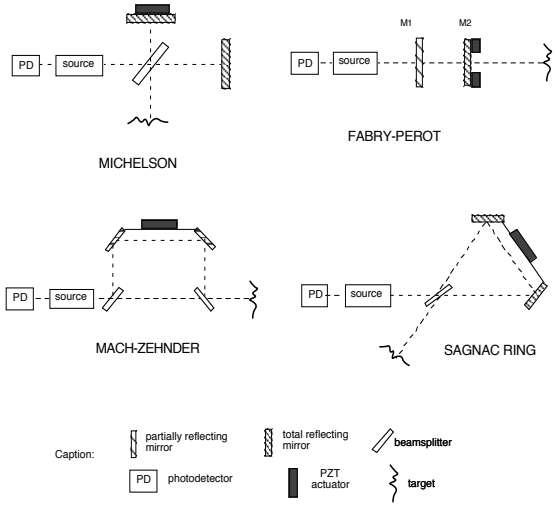


Fig.5. Steep-edge filters for the FM-to-AM conversion of SMI signals can be implemented by different configurations of interferometers, like the Michelson, Fabry-Perot, Mach-Zehnder, and Sagnac Ring shown here. The schematics are exemplary of the *in-line* setup using *micro-optics* (or *bulk-optics*) technology (adapted from [4]).

The response of the FP-I and the SR-I is:

$$P(\nu) = P_0 /(1+F^2 \sin^2 2\pi\nu nd/c) \qquad (19B)$$

where d is the mirror spacing for the FP-I, and half the perimeter for the SR-I, and $F$ is the finesse, given by $F = 2r_1r_2/(1-r_1r_2)$ [4] in term of the mirror (field) reflectivity for the M-I, and $F = 2t/(1-t)$ for the SR-I (t being the field "bar" coupling factor).

Correspondingly, the maximum slope, obtained by differentiating Eq.19B is found as:

$$S_F = 2\pi (sn/c)\ \tfrac{1}{2}(F^2-1)^{1/2}$$
$$= 2\pi (sn/c)\ \tfrac{1}{2} F \quad (\text{for } F \gg 1) \qquad (20B)$$

Thus, at equal physical lengths ($\Delta L = d$), the FP-I and SR-I provide a slope $\approx \tfrac{1}{2} F$ times larger than MZ-I and M-I.

On choosing the filter, large slope is not the sole parameter of interest, however. Several features like back-reflection, number of arms, number of beam splitters and mirrors, etc., as summarized in Table I, shall be taken into account in the practical implementation.

For example, because of the back-reflection, M-I and FP-I filters should be preferred in the off-line configuration, whereas the MZ-I and SR-I filters are suitable also for the in-line configuration.

Table I Comparison of interferometer-based filters

| | M-I | FP-I | MZ-I | SR-I |
|---|---|---|---|---|
| Responsivity | 2 | *F* | 1 | *F* |
| Back-reflection to source | yes | yes | no | no |
| No. of arms | 2 | 1 | 2 | 1 |
| Reference available | yes | no | yes | no |
| No. of beam splitters (or partially refl. mirrors) | 1 | 1 | 2 | 1 |
| Metallization required (for fiber versions) | 2 | 2 | 0 | 0 |

Notes: The M-I and the FP-I can have source and detector on the same side if the output is taken by a beam splitter added on the input path. Back-reflection is for the basic configuration with mirrors; using corner cubes, it is avoided in the Michelson.

Tuning of the resonance is readily implemented in M-I and FP-I filters by means of a PZT actuator mounted on a mirror (as shown in Fig.5), whereas for MZ-I and SR-I filters we either need to insert a phase modulator in the propagation path, or to collapse two mirrors into a double total-reflection prism (as hinted in Fig.5) to allow the PZT actuator change the path length while maintaining alignment of the interferometer.

About technology, in addition to the *bulk- (or micro-) optics* configurations shown in Fig.5 we can use the corresponding *all-fiber* versions, as exemplified in Fig.6 in the case on the *off-line* placement of the filter. [Obviously, we may have also the *all-fiber in-line* and the *micro-optics off-line* configurations, whose schematics are omitted here to save space].

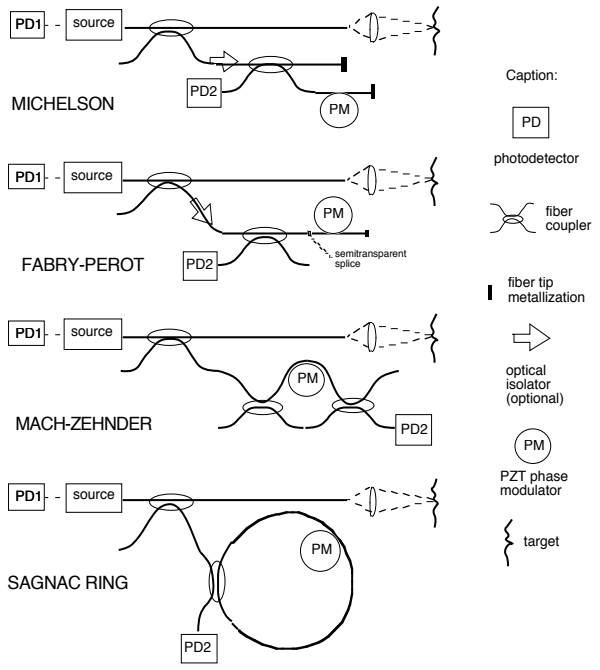


Fig.6 same as Fig.5, but here the interferometers are here implemented with the *all-fiber* technology and exemplary of the *off-line* placement of the filter (adapted from [4]).

For example, as developed in [22], using an unbalance of $\Delta L$=60-cm, and taking n=1.5 for the fiber, Eq.20A gives $S_F$=19 $GHz^{-1}$. The phase modulator (PM) was realized by a PZT cylinder with a few turns of fiber wound on it, and it allowed to tune the filter to the laser wavelength on several FSR (free spectral range) of the filter. By a servo loop, the working point of the MZ-I filter was locked at half the maximum power of the SMI signal (i.e., at half-fringe), where we find the largest slope of the MZ-I filter.

## VI. APPLICATIONS

Several applications may benefit from the increased signal amplitude and SNR offered by the converted FM signal, when used in place of the usual AM signal, and this applies to both the on-line or off-line configurations. Even more important, the simultaneous availability of CFM and AM signals allows to cover new applications for the laser diode SMI, equaling those of the He-Ne dual mode laser. Below we list three examples (yet not exhaustive) exploiting the use of the CFM signal.

### *VIa - Measurements of Sub-Wavelength Amplitude of Vibration*

Interferometry is a well-known technique for analogue measurement of sub-wavelength amplitude of vibration [2]. When specialized to the SMI configuration, it takes the form of a servo loop locking the SMI at half-fringe, realized by means of a feedback loop including photodiode preamplifier, differential amplifier, voltage-to-current converter and laser bias-current feed [2,4,45,46], so that the SMI signal $\cos 2k(\Delta s+\lambda/4)$ becomes $-\sin 2k\Delta s \approx -2k\Delta s$, or, it is linear for small amplitudes $\Delta s$. Readout of the signal is available at the difference amplifier output [45], and the dynamic range is nicely expanded (up to several mm) because of the feedback effect, while the minimum detectable signal is found experimentally to go down to typically 50…100 pm/√Hz [46].

Theoretically, we can repeat the arguments developed in Sect. II A to evaluate the minimum detectable $\Delta s$ or NED (noise equivalent displacement) [4] of the SMI vibrometer. We start considering of an SMI signal of the type

$$P = P_0 [1+V\cos 2k(\Delta s+\lambda/4)] \qquad (21)$$

where V is the fringe visibility or, equivalently, the modulation depth $2\kappa C$ of the SMI signal (Eq.7).

The NED is given by the phase noise $\varphi_n$ [on its turn given by the inverse of the $SNR_{AM}=2\kappa C/\sqrt{(P/2h\nu B)}$ of the amplitude measurement], divided by 2k [4], so that we can write

$$NED = (\lambda/4\pi)/SNR_{AM} = (\lambda/4\pi)\,(2h\nu B/VP_0)^{1/2}/2\kappa C \qquad (22)$$

where B is the measurement bandwidth and $P_0$ is the received optical power carrying the SMI signal.

Using the converted FM signal in place of the usual AM signal, Eq.22 would become $NED = (\lambda/4\pi)/SNR_{CFM}$ or, we get an improvement of NED just given by the factor $G_{SNR}= SNR_{CFM}/SNR_{AM}$. Should the source of the vibrometer be the laser presented in Ref. [21], for which a gain $G_{SNR}$=87.5 has been measured, then the attainable NED would drop from the reference 50...100 pm/√Hz to 0.56…1.13 pm/√Hz, a quite

interesting value. A similar result would be obtained with the setup of Ref. [22], reporting a factor 149 of SNR improvement with a 20-mW laser source: in this case the NED would drop to 0.33…0.66 pm/√Hz.

Yet, we should consider that the above powers are rather large respect to those normally employed for safety issues in a laser vibrometer.

So, let us now we evaluate the improvement for the realistic case, i.e., for a wavelength $\lambda$=850-nm, a power $P_{out}$=5-mW, of which 10% used in the off-line branch FM converter, a preamplifier bandwidth B=1-Hz, and a distance s=60-cm, like in the design of the vibrometer in Refs. [45,46] attaining a record low 20-pm/√Hz.

With the numerical values of Sect. III, we get form Eqs.2-8: $\eta_s=\eta_m \lambda/\pi w_t=0.4\cdot10^{-3}$, being $w_t$=0.4-mm at s=60-cm, and the C factor is slightly less than one, C=0.535, in accordance with the moderate regime of feedback observed experimentally [46]. Then, from Eqs.12-15 we find $SNR_{AM}$=2430.

From Eq.22, this SNR corresponds to a minimum detectable displacement NED=25.9-pm for the AM channel, in agreement with the 20-pm of the experiment reported in [46].

On the other side, using the CFM channel we find $SNR_{CFM}$=7.2, so there will be no advantage in using it at 1-Hz bandwidth and with a 5-mW power.

But, if the vibration signal is fast, like in the application to acoustic emission, and we expand the bandwidth to B=1-MHz, then $SNR_{AM}$ will drop to 2.43 while $SNR_{CFM}$ is still 7.2, so we have an advantage in sensitivity of a factor 3 over the NED=25.9 -nm of the AM channel. Even more, using $P_{out}$=50-mW (and $P_0$=5-mW) we would add another factor √10, and the improvement becomes 9.5, so that the minimum displacement measurable at B=1-MHz would go down to NED=2.7-nm, a quite interesting result.

Another application sharing the same problems of vibrometers is the detection of single micro-particles in a gas flow, successfully reported in Ref. [48].

*VIb- Two Channels Displacement Measurements*

As introduced in early papers on SMI [1,4], the availability of two orthogonal signals cos2ks and sin2ks allows to trace back the displacement s(t) without the ambiguity caused by movement reversals [19]. The digital readout of the SMI signals easily follows, and consists in up/down counting the semi-periods of both cos and sin waveforms at their zero-crossings, looking at the polarity of the other signal to decide the sign of the count. As there are two zero-crossings per period in each waveform and the period corresponds to a $\lambda$/2-displacement, this SMI is a digital readout instrument with a LSB $\lambda$/8-resolution [4], i.e., 79-nm for a $\lambda$=633-nm He-Ne laser, as developed in [1].

With the new, converted-FM SMI channel becoming available, we can apply the above mode of operation also to a semiconductor laser source. The only problem is that the AM and CFM signals are not really orthogonal, as we can see from Eqs.3 and 4. In power, they are written as:

$$\Delta P_{AM}= P_0\ \kappa C \cos 2ks \qquad (23A)$$

$$\Delta P_{CFM}= P_0\ \sigma_F\,(C/\tau_{ext})\ \sin(2ks+\operatorname{atan}\alpha) \qquad (23B)$$

After a scale factor adjustment to bring the amplitudes $\kappa$C and $\sigma_F\,(C/\tau_{ext})$ to the same value $A=\kappa C(\sigma_F/\tau_{ext})$ [by multiplying the first by $(\sigma_F/\tau_{ext})$ and the second by $\kappa$] we can make an orthogonalization by sum and difference, generating signals $\Sigma$ and $\Delta$:

$$\Sigma = A\,[\cos 2ks + \sin(2ks+\operatorname{atan}\alpha)] =$$
$$= 2A\cos(2ks-\pi/4+\tfrac{1}{2}\operatorname{atan}\alpha)\sin(\pi/4+\tfrac{1}{2}\operatorname{atan}\alpha) \qquad (24A)$$

$$\Delta = A\,[\cos 2ks - \sin(2ks+\operatorname{atan}\alpha)] =$$
$$= -2A\sin(2ks-\pi/4+\tfrac{1}{2}\operatorname{atan}\alpha)\cos(\pi/4+\tfrac{1}{2}\operatorname{atan}\alpha) \qquad (24B)$$

Now, $\Sigma$ and $\Delta$ contain cos and sin of the same argument, so they are orthogonal, and by processing them as outlined above for the He-Ne laser, the displacement s(t) can be measured in $\lambda$/8 steps. The schematic needed to implement the idea is reported in textbooks (see e.g., Ref. [47]) and we omit it here to save space.

A problem now arises: for the orthogonalisation to be effective, we need the alpha factor be not very high, because for large $\alpha$ the term ½atan $\alpha$ in Eq.24 becomes $\pi$/4, and the amplitude $\cos(\pi/4+\tfrac{1}{2}\operatorname{atan}\alpha)$ of signal $\Delta$ vanishes, as indicated by Eq.24B. The other the multiplicative term, of $\Sigma$ in Eq.24A poses no problem, because $\sin(\pi/4+\tfrac{1}{2}\operatorname{atan}\alpha)$ is around unity for large $\alpha$.

Let's now evaluate the minimum SNR (or the maximum $\alpha$-factor) that makes $\Delta$ still usable. At large $\alpha$, from Eq.24B signal $\Delta$ is reduced by a factor $\cos(\pi/4+\tfrac{1}{2}\operatorname{atan}\alpha) \approx 2/\alpha$ [an approximation good to <5% already at $\alpha$>2.5], while $\Sigma$ is unaffected.

Thus, the $SNR_\Sigma$ of $\Sigma$ is the composition of SNR of the two cos and sin addenda in Eq.24A, which are the $SNR_{AM}$ and $SNR_{CFM}$. With easy algebra we find for the result:

$$SNR_\Sigma = SNR_{AM}\ SNR_{CFM}/(SNR_{AM}^2+SNR_{CFM}^2)^{1/2} \qquad (25)$$

This is the SNR of $\Sigma$, whereas for $\Delta$ we have a signal $2/\alpha$ times (for large $\alpha$) the amplitude A, so we have:

$$SNR_\Delta = 2\ SNR_\Sigma/\alpha \qquad (26)$$

To be able resolve the $\lambda$/8 count in the displacement measurement, we need NED= $\lambda$/8, and equating (Eq.22) to the NEDs of $\Sigma$ and $\Delta$, $NED=(\lambda/4\pi)/SNR_{\Sigma,\Delta}$, we find the required SNRs as:

$$SNR_\Sigma = 2/\pi, \qquad SNR_\Delta = 4\alpha/\pi \qquad (27)$$

Thus, the requirement is not so demanding, in view of the numerical evaluations of Sect. II, or, the $\lambda$/8 count resolution can be easily obtained even at large $\alpha$-factors, like $\alpha$=6.

*VIc - Alpha Factor Measurements*

The line-width enhancement factor, or alpha-factor, introduced by Henry [49] is important in semiconductor lasers as it determines how much amplitude noise is transferred into frequency noise [50], and for this reason the $\alpha$ is introduced as

a multiplicative factor in the second of the Lang and Kobayashi equations (Eq.1). A number of different methods have been proposed for the measurement of the alpha factor, and Ref. [51] presents an account of the outcomes found on applying them in a round robin test. Along with methods that are rather complicate, the original proposal based on SMI [11] is much simpler and easy to carry out experimentally. It is based on the analysis of the self-mixing waveform generated by a sinusoid driven target, and we look at waveform details like zero crossing and edge switching times. To apply the method, we only need C>1, that is, to operate in the moderate coupling regime.

Now that we have available both AM and FM signals, which are phase shifted of $\zeta = \pi/2 - \text{atan}\ \alpha$ (Eq.5), the measurement of the $\alpha$-factor is even simpler and also feasible at in the weak coupling regime (C<1), because we just have to measure the phase-shift between AM and FM signals, $\arg(\Delta E) - \arg(\Delta \nu) = \zeta$ to trace back $\alpha$ fromEq.5.

About accuracy, a small error $\Delta\zeta$ in phase-shift measurement will determine a $\Delta\alpha$ error in alpha factor, which can be found by differentiating the inverse function of Eq.5 with the result:

$$\Delta\alpha = (d\alpha/d\zeta)\,\Delta\zeta = -(1+\alpha^2)\,\Delta\zeta \qquad (28)$$

The phase-shift error is contributed by three terms: (i) phase-shift unbalance of the electronic circuits handling the photo-detected SMI signal, a deterministic error $\Delta\zeta_{det}$ that should be carefully trimmed to zero, (ii) the error $\Delta\zeta_{mic}$ due to stray vibrations collected by microphonics, and (iii) the phase noise of the two (AM and CFM) channels. Phase noise is the inverse of the SNR of the amplitude, $SNR_P = [P_{AM}/2h\nu FB]^{1/2}$ for a signal power $P_0$ on a bandwidth B, and this is the contribution for the AM channel (Eq. 12), while for the CFM the SNR is $G_{SNR} = SNR_{CFM} / SNR_{AM}$ times larger (Eq.16).

Summing up (as squares) the two contributions, the total phase noise fluctuation $\Delta\zeta_n$ is:

$$\Delta\zeta_n = [P_0(1+1/G_{SNR}^2)/2h\nu FB]^{-1/2} \qquad (29)$$

where, as soon as it is $G_{SNR} >> 1$, the CFM contribution becomes negligible and this term can be dropped from Eq.29.

With the data of Sect. II, we find the maximum measurable alpha by equating $\Delta\zeta_n$ to $\pi/2 - \text{atan}\ \alpha$, and the result is $\alpha_{max}=700$, a very high limit indeed.

## CONCLUSIONS

We have pointed out the usefulness of the FM channel in the measurements with SMI, and evaluated the theoretical improvement obtained in signal amplitude and SNR respect to the AM channel. Some configurations to implement the FM-to-AM conversion have been discussed and finally we have hinted several applications with improved performance.

## REFERENCES


[1] S. Donati, “Laser Interferometry by Induced Modulation of the Cavity Field”, *Journal Appl. Phys.*, vol.49 (1978), pp.495-497.

[2] S. Donati: ”Developing Self-Mixing Interferometry for Instrumentation and Measurements” *Laser Photonics Rev*. vol.6 (2012), pp. 393–417 (DOI) 10.1002/ lpor.201100002.

[3] G.Giuliani, M. Norgia, S. Donati, T.Bosch: ‘Laser Diode Self-Mixing Technique for Sensing Applications’, *J. of Optics A,* vol.4, (2002), pp.S283-S294.

[4] S. Donati: “*Electrooptical Instrumentation*”, Prentice Hall, Upper Saddle River, N.J., 2004, Chapter 4.

[5] S. Donati: “Responsivity and Noise of Self-Mixing Photodetection Schemes”, *IEEE Journal Quantum El*., vol.47, 2011, pp.1428-1433.

[6] S. Donati, M. Sorel: “A Phase-Modulated Feedback Method for Testing Optical Isolators Assembled in the Laser Package”, *IEEE Photonics Techn. Lett.*, vol. 8 (1996), pp. 405-408.

[7] P.Dean, Y.L.Lim, A.Valavanis, R.Kleise, M.Nikolic, S.P.Khanna, M.Lachab, D.Indjin, Z.Ikonic, P.Harrison, A.D.Rakic, E.H.Lindfield, G.Davies: “Terahertz Imaging through Self-Mixing in a Quantum Cascade Laser”, *Opt. Lett.* vol.36, pp.2587-2589 (2011).

[8] P.Dean, A.Valavanis, J.Keeley, K.Berting, Y.L.Lim, R.Alhathool, S.Chowdury, T.Taimre, L.H.Li, D.Indjin, S.Wilson, A.D.Rakic, E.H.Linfield and A.G.Davies: "Coherent three-dimensional terahertz imaging through self-mixing in a quantum cascade laser" *Appl. Phys. Lett.,* vol.103 (2013) DOI 181112.

[9] M.Fathi, S.Donati: “Thickness Measurement of Transparent Plates by a Self-Mix Interferometer”, *Optics Letters*, vol.35, 2010, pp.1844-46.

[10] G.Giuliani, M. Norgia: ‘Laser Diode Linewidth Measurement by means of Self-Mixing Interferometry’, *IEEE Phot. Techn. Lett*., vol.PTL-12 pp.1028-1030. (2000)

[11] Y. Yu, G. Giuliani, S. Donati, "Measurement of the Linewidth Enhancement Factor of Semiconductor Lasers by Self-Mixing Effect", *IEEE Photon. Technol. Lett*., vol.16, pp. 990-992 (2004).

[12] J.Xi, Y.Yu, J.F.Chicaro and T.Bosch: "Estimating the parameters of Semiconductor lasers Based on Weak Optical Feedback Self-Mixing Interferometry" *IEEE J. Quant. Electr.,* vol.41 (2005), pp.1058-1064.

[13] R.Kliese, T.Taimre, A.Bakar, Y.L.Lim, K.Bertling, M.Nikolic, J.Perchoux, T.Bosch and A.D.Rakic: "Solving Self-mixing Equations for Arbitrary Feedback Level: A Concise Algorithm", *Appl. Optics* vol.53 (2014), pp.3723-3736.

[14] S. Donati, V. Annovazzi Lodi, S. Merlo, and M. Norgia, “Measurements of MEMS Mechanical parameters by Injection Interferometry”, *Proc. IEEE-LEOS Conf. Optical MEMS*, Kawai, HI, 21-24 Aug.2000, pp.89-90, see also: *IEEE Transaction on Mechatronics*, vol.6 (2001), pp.1-6.

[15] R. Atashkooei, J.C Urresty, S. Royo, J.R.Riba and L.Romeral: "Runout tracking in electrical motors using self-mixing interferometry", *IEEE Trans. Mechatronics*, vol.19 (2014), pp. 184-190.

[16] S. Donati, M.Norgia: "Self-mixing Interferometry for Biomedical Signals Sensing" (invited paper), *IEEE Journal Select. Topics Quantum El*. vol.20, 2014, DOI 10.1109/JSTQE.2013.2270279

[17] A.Arasanz, F.J.Azcona, S.Royo, A.Jha and J.Padellorens: "A new method for the acquisition of arterial pulse wave using self-mixing interferometry", *Opt. and Laser Techn*. vol.63 (2014), pp.98-104

[18] Philips NV (Eindhoven): "*Twin Eye Laser Sensor"* (SMI integrated chip), see http://www.photonics.philips.com/application-areas/sensing (2011)

[19] S. Donati, G. Giuliani, S.Merlo: "Laser Diode Feedback Interferometer for Measurement of Displacement without Ambiguity", *IEEE Journal of Quantum Electronics*, vol. QE-31 (1995), pp.113-119.

[20] see Ch.7.5 of Ref.[4] for a similar solution in the context of Sagnac phase measurement.

[21] V.Contreras, J.Lonnquist and J.Toivonen: "Edge Filter Enhanced Self-Mixing Interferometry", Opt. Lett. vol.40, 2015, pp.2814-2817.

[22] M.Norgia, D.Melchionni, S.Donati: “Exploiting the FM-signal in a laser-diode SMI by means of a Mach-Zehnder filter”, *IEEE Phot. Techn. Lett*., vol.PTL-29 (2017), in press.

[23] R. Lang and K. Kobayashi, “External Optical Feedback Effects on Semiconductor Injection Laser Properties”, *IEEE J. Quant. Electr.*, vol.QE-16 (1980), pp.347-355.

[24] S.Donati: "*Photodetectors"*, Prentice Hall 1999, Chapter 3.

[25] P.W.Milonni and J.H.Eberly: "*Laser Physics*", J.Wiley and Sons, New Your 2010, see Eq.5.11.13 on p.205 and Eq.5.11.16 on p.206.

[26] R. Paschotta, H. R. Telle, and U. Keller, “Noise of Solid State Lasers”, in *Solid-State Lasers and Applications* (ed. A. Sennaroglu), CRC Press, Boca Raton, FL (2007), Chapter 12, pp. 473–510, see also: "Derivation of the Schawlow-Townes Linewidth of Lasers" https://www.rp-photonics.com/Schawlow-Townes_ linewidth. pdf .

[27] M. Lax, “Classical Noise. V. Noise in Self-Sustained Oscillators”, *Phys. Rev.* vol.160 (2), 290 (1967) This paper corrects the Schawlow-Townes limit by factor ½.

[28] O.Svelto: "Principles of Lasers", 4th ed., Springer, Berlin 1998.

[29] P.-Y. Ho: ”Phase and Amplitude Fluctuations in a Mode-Locked Laser”, *IEEE J. Quant. Electronics*, QE-21 (1985) pp. 1806-1813.

[30] D. Allan: "Statistics of Atomic Frequency Standards", *Proceedings of IEEE,* vol. 54 (1966) pp. 221–230.

[31] G.DiDomenico, S.Schilt, and P.Thomann: "Simple Approach to the Relation between Laser Frequency Noise and lase Line Shape, *Appl. Optics*, vol.49 (2010), pp.4801-4807.

[32] P.Laurent, A.Clairon, and C.Breant: "Frequency Noise Analysis of Optically Self-Locked Diode Laser", *IEEE J. Quant. El.*, vol.25 (1989) pp.1131-1142.

[33] R. W. Tkach and A. R. Chraplyvy: “Regimes of Feedback Effects in 1.5-um Distributed Feedback Laser” *IEEE J. Lightwave Technol.*, LT-4, (1986), pp. 1655-1661.

[34] S. Donati, S.-K. Hwang: "Chaos and High-Level Dynamics in Coupled Lasers and their Applications", *Progress in Quantum Electronics* (2012), vol.36, Issues 2-3, March/May 2012, pp. 293–341.

[35] S. Donati, R.-H-.Horng: "The Diagram of Feedback Regimes Revisited", *IEEE Journal Select. Topics Quantum El.* vol.19, 2013, pp. DOI 10.1109/JSTQE.2012.2234445.

[36] K. Petermann: "External Optical Feedback Phenomena in Semi-conductor Lasers", *IEEE J. Select. Topics Quant. El.*, vol.1, 1995, pp.480-489.

[37] N.Schunk and K.Petermann: "Stability Analysis of Laser Diodes with Short External Cavity", *IEEE Photonics Techn. Lett.,* vol.LT-1, 1989, pp.49-51.

[38] K. Petermann: “*Laser Diode Modulation and Noise*”, Kluwer Academic Publ., Dodrecht, 1991.

[39] J. Ohtsubo: "Semiconductor Lasers - Stability, Instability and Chaos" 2nd ed., Springer, Berlin 2008.

[40] G.Agrawal: "Line Narrowing in a Single-Mode Injection Laser Due to External Optical Feedback", *IEEE Journal Quantum El.* vol.QE-20, 194, pp468-471.

[41] G. Duan, P. Gallion, G. Debarge: "Analysis of frequency chirping of semiconductor lasers in the presence of optical feedback" *Appl. Optics* vol.12, 1987, pp.800-802.

[42] S. Donati, M.T.Fathi: "Transition from Short-to-Long Cavity and from Self-Mixing to Chaos in a Delayed Optical Feedback Laser", *IEEE Journal Quantum El.* vol.QE-48, 2012 , pp.1352-1359.

[43] S.Donati, D.Rossi, M.Norgia: "Single Channel Self-Mixing Interferometer Measures Simultaneously Displacement and Tilt and Yaw Angles of a Reflective Target", *IEEE Journal Quantum El.*, vol. QE-51, 2015, DOI 1400108.

[44] Kanaev, I.F., Malinovskii, V.K. & Surovtsev: "Narrow-band holographic interference $LiNbO_3$-based filters", N.V. Phys. Solid State (2000) 42: 2142. doi:10.1134/1.1324054

[45] G.Giuliani, S.Bozzi-Pietra, S. Donati: 'Self-Mixing Laser Diode Vibrometer', *Meas. Science and Techn.*, vol.14 (2003), pp.24-32.

[46] S.Donati, M. Norgia, and G. Giuliani: “Self-mixing differential vibrometer based on electronic channel subtraction” *Applied Optics*, vol. 45 (2006), pp. 7264-7268

[47] see Chapter 4.2, pp. 96-99 of Ref.[4]

[48] V.Contreras, J.Lonnquist and J.Toivonen: "Detection of single microparticles in airflows by edge-filter enhanced self-mixing interferometry", *Opt.Expr*.vol.24 (2016), pp.8886-8894.

[49] C. H. Henry, **“**Theory of the linewidth of semiconductor lasers,**”** *IEEE J. Quantum Electron.*, vol. QE-18, pp. 259–264, Feb. 1982.

[50] M. Osinski and J. Buus, **“**Linewidth broadening factor in semiconductor lasers-an overview,**”** *IEEE J. Quant. Electr.,* vol. QE-23, (1987)pp.9–28.

[51] A. Villafranca, G.Giuliani, S.Donati, et al.: "*Linewidth Enhancement Factor of Semiconductor Lasers: Results from Round Robin in COST 288*", CLEO Baltimore, May 6-11, 2007, paper CThK-1.


**Silvano Donati** (M’75, SM’98, F’03, LF’09) earned his doctorate in Physics (Laurea in Fisica) *cum laude* from University of Milan, Italy, 1966, and has been Chair Professor of University of Pavia from 1980 to 2010, and Lecturer from 2010 to 2014 before becoming Emeritus Professor in 2015. He has authored or co-authored 300+ papers and holds a dozen patents. He has introduced self-mixing interferometry and chaos-shift-keying cryptography, the topics covered in his Distinguished Lecture talk given in 21 LEOS (now IPS) Chapters in two terms, 2007/08 and 2008/09. He has received several awards from the AEIT and IEEE, in particular the Marconi medal of AEIT, the Aaron Kressel Award and the Distinguished Service Award of the IEEE Photonics Society. He has authored two books, ‘Photodetectors’ (Prentice Hall, 1999) and ‘Electro-Optical Instrumentation’ (Prentice Hall, 2004). He was the founder (1996) and first Chairman (1997-01) of the Italian LEOS Chapter, LEOS VP Region 8 Membership (2002-04) and BoG (2004-06), and the Chairman of the IEEE Italy Section (2008-09). He has been invited as Visiting Professor at several Universities of Taiwan: NTU, Taipei, 2005, Sun Yat Sen, Kaohsiung (2007, 2008, 2010), NCKU, Tainan 2012, NCHU, Taichung, 2013-14, and NTUT, Taipei 2015-6. He is also Associate of the Italian Institute of Optics (ISASI) of the National Science Foundation (CNR). Prof. Donati is Life Fellow of the IEEE, and OSA Emeritus Fellow.

Michele Norgia (S'99-M’01-SM’09) was born in Omegna, Italy, in 1972. He received the M.S. degree with honours in Electronics Engineering from the University of Pavia in 1996 and in 2000 he received the Ph.D. degree in Electronics Engineering and Computer Science. In 2006, he joined the Electronic and Information Science Department of the Politecnico di Milano, and in 2014 he was appointed to the position of Associate Professor. His main research interests are optical and electronic measurements, interferometry, chaos in lasers, micro-electro-mechanical sensors and biomedical measurements. He is author of more than 150 papers published in international journals or conference proceedings. Dr. Norgia is a member of the Italian Association “Group of Electrical and Electronic Measurements” and a senior member of IEEE.